Development 137, 3221-3231 (2010) doi:10.1242/dev.054668

Inhibition of Wnt signaling by Wise (Sostdc1) and negative feedback from Shh controls tooth number and patterning

Youngwook Ahn[1], Brian W. Sanderson[1], Ophir D. Klein[2] and Robb Krumlauf[1,3,*]

SUMMARY

Mice carrying mutations in *Wise* (*Sostdc1*) display defects in many aspects of tooth development, including tooth number, size and cusp pattern. To understand the basis of these defects, we have investigated the pathways modulated by Wise in tooth development. We present evidence that, in tooth development, Wise suppresses survival of the diastema or incisor vestigial buds by serving as an inhibitor of Lrp5- and Lrp6-dependent Wnt signaling. Reducing the dosage of the Wnt co-receptor genes *Lrp5* and *Lrp6* rescues the *Wise*-null tooth phenotypes. Inactivation of *Wise* leads to elevated Wnt signaling and, as a consequence, vestigial tooth buds in the normally toothless diastema region display increased proliferation and continuous development to form supernumerary teeth. Conversely, gain-of-function studies show that ectopic Wise reduces Wnt signaling and tooth number. Our analyses demonstrate that the Fgf and Shh pathways are major downstream targets of Wise-regulated Wnt signaling. Furthermore, our experiments revealed that *Shh* acts as a negative-feedback regulator of Wnt signaling and thus determines the fate of the vestigial buds and later tooth patterning. These data provide insight into the mechanisms that control Wnt signaling in tooth development and into how crosstalk among signaling pathways controls tooth number and morphogenesis.

KEY WORDS: Wnt signaling, Shh, Fgf, Wnt antagonists, Feedback regulation, Tooth development, Mouse

INTRODUCTION

The extensive variation in tooth number and morphology in vertebrates raises important questions about how patterning of dentition is controlled during evolution and development. In mammals, teeth develop sequentially in an anterior-to-posterior direction. The initiation of tooth development is characterized by thickening of the oral ectoderm and subsequent condensation of neural-crest-derived mesenchyme around the invaginating epithelium to form tooth buds (Tucker and Sharpe, 2004). Signaling between the dental epithelium and mesenchyme modulates the survival and growth of tooth buds. This signaling is crucial for determining tooth number, as rudimentary or vestigial buds initially form in the toothless diastema region between the incisors and molars but degenerate without reaching the cap stage (Peterkova et al., 2006). At the beginning of the cap stage, a transient epithelial signaling center, called the enamel knot, is induced at the tip of the tooth bud and it regulates tooth growth and morphogenesis (Tucker and Sharpe, 2004).

Mutations in a number of genes encoding components of major signaling pathways have been shown to influence tooth number. This is consistent with the idea that crosstalk between several major signaling pathways, such as Fgf, Shh, Wnt and Bmp, regulates tissue interactions and modulates tooth formation (Tummers and Thesleff, 2009). Many of these pathways are reiteratively used at different stages of tooth development. In the case of Wnt signaling, tooth development is arrested at the early bud stage when Wnt signaling is inactivated, either by conditional knockout of β-catenin or by overexpression of the Wnt antagonist dickkopf 1 (*Dkk1*) in the dental epithelium (Andl et al., 2002; Liu et al., 2008). Conversely, ectopic Wnt activation leads to supernumerary teeth as well as abnormal cusp patterning (Jarvinen et al., 2006; Wang et al., 2009). Therefore, tight control of Wnt signaling activity is essential for normal tooth development, yet it is unclear how this control is achieved and how Wnt signaling interacts with other signaling pathways during tooth development.

Wise (also known as *Sostdc1*, *ectodin* and *USAG-1*) was identified in a functional screen as a gene encoding a conserved secreted protein capable of modulating canonical Wnt signaling (Itasaki et al., 2003). In vitro assays revealed that Wise and the closely related Sost protein bind to the extracellular domain of the Wnt co-receptors Lrp5 and Lrp6 and inhibit Wnt signaling (Ellies and Krumlauf, 2006; Itasaki et al., 2003; Li et al., 2005; Lintern et al., 2009; Semenov et al., 2005). In vitro assays have also revealed that Wise can bind to the extracellular domain of the related Lrp4 receptor (Ohazama et al., 2008). Based on mutations of *Lrp4* in humans and mice, it has been postulated that Lrp4 can modulate Wnt signaling mediated by Lrp5 and Lrp6 (Choi et al., 2009; Li et al., 2010; Ohazama et al., 2008; Weatherbee et al., 2006). In addition, Wise is phylogenetically related to several subgroups of Bmp antagonists within the cystine-knot superfamily, and Wise has been shown to bind to a subset of Bmps in vitro and to influence Bmp signaling (Laurikkala et al., 2003). Therefore, Wise has the potential to provide multiple regulatory inputs into Lrp5/6, Bmp- and Lrp4-dependent pathways.

Wise loss-of-function mutants display defects in many aspects of tooth development including tooth number, size and cusp pattern (Kassai et al., 2005; Yanagita et al., 2006). Loss of *Wise* can increase the sensitivity to excess Bmp in cultured teeth, suggesting that Wise might have a function as a Bmp antagonist in teeth (Kassai et al., 2005). Mice homozygous for a hypomorphic allele of *Lrp4* displayed tooth defects similar to those of *Wise*-null mice,

[1]Stowers Institute for Medical Research, Kansas City, MO 64110, USA. [2]Departments of Orofacial Sciences and Pediatrics, Program in Craniofacial and Mesenchymal Biology, University of California at San Francisco, San Francisco, CA 94143-0442, USA. [3]Department of Anatomy and Cell Biology, University of Kansas Medical Center, Kansas City, KS 66160, USA.

*Author for correspondence (rek@stowers.org)

Accepted 14 July 2010

suggesting that they might cooperate in regulating Wnt signaling (Ohazama et al., 2008). Furthermore, a recent study with cultured *Wise*-deficient incisors suggested that Wise from the dental mesenchyme can limit tooth formation via inhibition of both Bmp and Wnt signaling (Munne et al., 2009). As signaling pathways play diverse roles at multiple stages of tooth development it is important to understand the stage- and process-specific mechanisms through which Wise exerts its in vivo regulatory activity.

In this study, we have used *Wise*-null mutants and a transgenic gain-of-function system to investigate crosstalk between signaling pathways and the molecular and cellular mechanisms that regulate the development and ultimately the number of teeth. We present genetic evidence that Wise inhibits Wnt signaling dependent upon the Wnt co-receptors Lrp5 and Lrp6 to suppress survival of vestigial buds in the incisor and molar regions. We found that the Fgf and Shh pathways are major downstream targets of Wise-regulated Wnt signaling and that Shh acts as a negative-feedback regulator of Wnt signaling during the bud-to-cap transition. Our data provide insight into how signaling pathways interact with each other to regulate cellular processes which govern key aspects of tooth formation.

MATERIALS AND METHODS

Mouse strains

Lrp5, *Lrp6*, *Top-Gal*, *Ctnnb1*$^{(ex3)fx}$, *Shh*^{GFPcre}, *Shh*^{creERT}, *Shh*^{neo}, *Shh*^{fx}, *Ptch1*^{LacZ}, *R26R*, *Fgfr1*, *Fgfr2*, *Fgf10*, *Bmpr1a* and *K14-Cre* mice were described previously (Chiang et al., 1996; DasGupta and Fuchs, 1999; Dassule et al., 2000; Harada et al., 1999; Harfe et al., 2004; Kato et al., 2002; Milenkovic et al., 1999; Min et al., 1998; Mishina et al., 2002; Pinson et al., 2000; Soriano, 1999; Trokovic et al., 2003; Yu et al., 2003). All experiments involving mice were approved by the Institutional Animal Care and Use Committee of the Stowers Institute for Medical Research (Protocol #2008-0002).

Generation of transgenic mice

To produce a *Wise-LacZ* BAC reporter, a *LacZ-SV40polyA* sequence was inserted in-frame into the first coding exon of *Wise* in a mouse BAC clone, RP23-166E23, which contains an 191 kb genomic region. BAC DNA was prepared using Qiagen Maxi-Prep Kit, linearized with PI-SceI and used for pronuclear injection into C57B6/JxCBA-F1 embryos.

A 2.2 kb promoter of the human keratin 14 gene was amplified from a BAC clone (RP11-434D2) using the primers 5′-AAGATCTAGG-TGCGTGGGGTTGGGATG-3′ and 5′-GAAGCTTGAGCGAGCAG-TTGGCTGAGTG-3′ and subcloned into the pCMS-EGFP vector (Clontech) replacing the CMV promoter. The mouse *Wise* cDNA was inserted downstream of the promoter. The 3.5 kb insert was gel-purified and injected into either C57B6/JxCBA-F1 or *Top-Gal* one-cell embryos.

β-gal staining, in situ hybridization and BrdU analysis

For β-gal staining, embryonic jaws were fixed in either 0.1% paraformaldehyde with 0.2% glutaraldehyde or 4% paraformaldehyde (PFA) for one hour on ice. After washing in phosphate-buffered saline, samples were stained in X-gal for 6-20 hours at room temperature. Wholemount in situ hybridization was performed with jaws fixed in 4% PFA according to standard protocols using DIG-labeled riboprobes. Cell proliferation was measured by injecting BrdU into pregnant females 2 hours before embryo harvest. Histological samples were paraffin-embedded, sectioned at 8 μm and stained with a rabbit caspase 3 antibody (Cell Signaling) or a mouse anti-BrdU antibody (Amersham). To induce Cre-recombination in *Shh*$^{+/CreERT}$ embryos, Tamoxifen was injected into pregnant females at the dose of 3-6 mg/40 g body weight.

qPCR arrays

Embryonic day (E) 13.5 tooth germs were dissected from 14 mandibles of *Wise*-null embryos and *Wise* heterozygous littermates. Total RNA was isolated and used for qPCR according to the manufacturer's protocol (SABiosciences). Four replicas were run for each signaling pathway array and the statistical analysis was performed using the software provided by the manufacturer. To compare gene expression between *Wise*$^{+/-}$ and *Wise*$^{+/-}$;*Shh*$^{+/-}$ tooth germs at E13.5, total RNA was extracted from six mandibular tooth germs for each genotype and four replicas were run with a TaqMan Array (Applied Biosystems).

RESULTS

Tooth phenotypes in *Wise*-null mice

We have used *Wise*-null mutants, which exhibit a variety of tooth defects, to investigate the genetic mechanisms that regulate the number and shape of teeth. Our *Wise*-null mice were generated by knock-in of a selection cassette into the first exon of the gene. Homozygous mutants displayed all the tooth abnormalities previously reported by other groups, including supernumerary incisors and molars, fused molars and cusp defects (Fig. 1; see Fig. S1A-F in the supplementary material) (Kassai et al., 2005; Yanagita et al., 2006). The maxillary molar region of *Wise*-null mice displayed extensive fusion of anterior teeth with full penetrance, resulting in two teeth in each jaw quadrant (Fig. 1B). In the mandibular molar region, there were two general phenotypes observed. In two-thirds of the animals, in place of the three molars (M_1-M_3) seen in control mice, four teeth (T_1-T_4) were observed in each jaw quadrant. In the remaining animals, we observed T_1-T_2 and/or T_2-T_3 fusions (Fig. 1B,H). We also observed a small extra tooth lateral to T_2 on the lingual side and a varying number of small teeth in the T_4 region (Fig. 1B). The frequency of the fusions and lateral teeth varied with strain backgrounds and was higher in C57BL6.

Genetic interactions between *Wise* and the Fgf and Bmp pathways

It is known that mutations in *Spry2* or *Spry4*, which are Fgf antagonists, result in formation of a premolar-like tooth due to elevated Fgf signaling and survival of a diastema bud (Klein et al., 2006; Peterkova et al., 2009). As the supernumerary teeth in the sprouty mutants were rescued by reducing dosage of genes encoding Fgf receptors (*Fgfr1* or *Fgfr2*) or ligands (*Fgf10*) (Klein et al., 2006), we attempted to rescue *Wise*-null tooth phenotypes through a similar strategy. However, the appearance of four molar teeth or supernumerary maxillary incisors in *Wise*-null mice was not affected in any of the compound mutant mice (see Fig. S1 in the supplementary material). Thus, modest reductions in Fgf signaling were not sufficient to compensate for the loss of *Wise* with respect to tooth number. As Wise has been implicated as a Bmp antagonist, we also attempted to rescue the *Wise* tooth phenotypes by reducing levels of Bmp signaling through removal of a copy of the *Bmpr1a* type I receptor gene. There were no significant changes in any of the phenotypes in *Wise*$^{-/-}$;*Bmpr1*$^{+/-}$ mice (see Fig. S1J,N in the supplementary material).

Dosage-dependent rescue of *Wise* tooth phenotypes by *Lrp5* and *Lrp6*

Wise has been implicated in modulation of the canonical Wnt signaling pathway through its ability to interact with the extracellular domain of the Lrp5 and Lrp6 co-receptors (Itasaki et al., 2003). We hypothesized that elevated Wnt signaling might account for abnormal tooth development in *Wise*-null mice. Therefore, we attempted to lower levels of Wnt signaling by reducing the dosage of the *Lrp5* and *Lrp6* co-receptor genes. Reduction in copies of *Lrp5* and/or *Lrp6* themselves did not result in tooth abnormalities (data not shown). However, in *Wise*-null

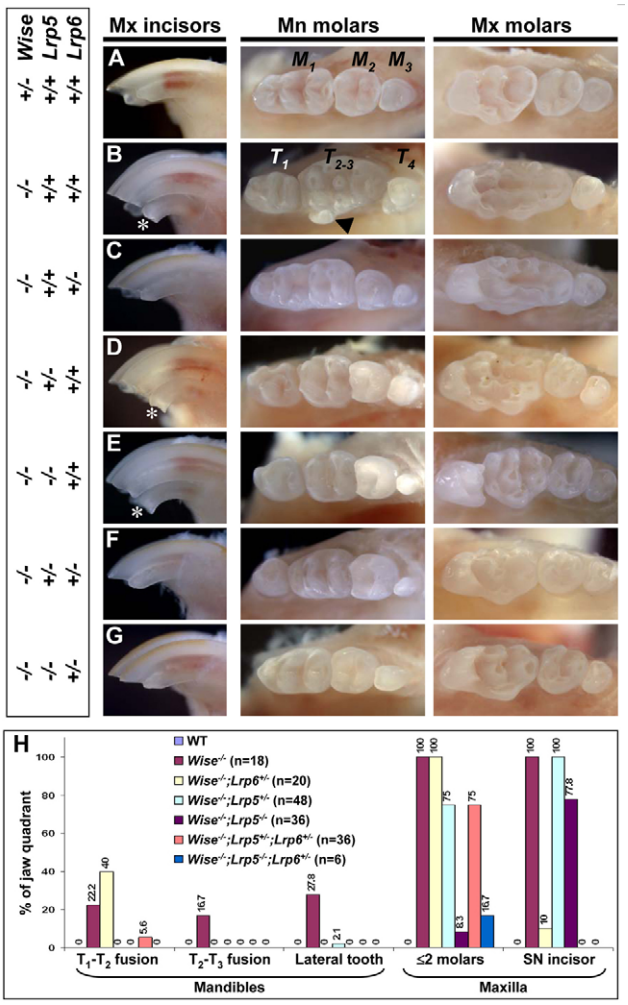

Fig. 1. Dosage-dependent rescue of *Wise* tooth phenotypes in *Lrp5* and *Lrp6* mutants. (**A-G**) Tooth phenotypes in *Wise*-null mutants carrying varying doses of the *Lrp5* and *Lrp6* Wnt-coreceptor genes. The genotypes are listed on the left and the respective incisor or molar regions noted at the top. M, molar; Mn, mandibular; Mx, maxillary; T, tooth. Asterisks mark the supernumerary incisor and the black arrowhead marks the supernumerary lateral molar. (**H**) Summary of the genetic interaction with the number of scored jaw quadrants shown as *n*. All phenotypes were scored with littermates in a mixed background of C57/BL6 and 129Sv/Ev. SN, supernumerary.

mice, we observed strong genetic interactions between *Wise* and *Lrp5* and *Lrp6*, as evidenced by rescue of all incisor and molar phenotypes.

Removal of only a single copy of *Lrp6* in *Wise*-null mice rescued both the supernumerary maxillary (90%) and mandibular (100%) incisor phenotypes (Fig. 1C,H; data not shown). *Lrp6*$^{-/-}$ mutants are embryonic lethal and hence we could not test this combination. Removing one copy of *Lrp5* had no effect (Fig. 1D,H), but in *Wise*$^{-/-}$;*Lrp5*$^{-/-}$ mice, supernumerary incisors were rescued in 22% of cases (Fig. 1E,H). When mice carried one or two *Lrp5*-null alleles in addition to an *Lrp6*-null allele, the supernumerary incisor phenotypes were completely rescued (Fig. 1G,H).

With respect to the abnormalities in the mandibular molars of *Wise*-null mice, removing one copy of either *Lrp5* or *Lrp6* rescued some aspects of the phenotype, as evidenced by the absence of a lateral supernumerary molar in 98% of cases (Fig. 1C,D). Although molar fusions completely disappeared in *Wise*$^{-/-}$;*Lrp5*$^{+/-}$ mice, only T_2-T_3 fusions were rescued in *Wise*$^{-/-}$;*Lrp6*$^{+/-}$ mice (Fig. 1H). Removing two of the four copies of the co-receptors resulted in a smaller T_1, but four molars were still present (Fig. 1E,F). Finally, in *Wise*$^{-/-}$;*Lrp5*$^{-/-}$;*Lrp6*$^{+/-}$ mice, the normal pattern of three molars in each jaw quadrant was restored in the majority of cases (5/6), including a fairly normal cusp pattern (Fig. 1G).

The maxillary molar region of *Wise*-null mice displayed two teeth in each jaw quadrant owing to extensive fusion of anterior teeth (Fig. 1B). Removing one copy of *Lrp6* had no effect on this fusion phenotype (Fig. 1C,H). However, the fusion phenotype was impacted by dosage of *Lrp5*, as three teeth were observed in 25% of *Wise*$^{-/-}$;*Lrp5*$^{+/-}$ mice and three or four teeth were observed in 92% of *Wise*$^{-/-}$;*Lrp5*$^{-/-}$ mice (Fig. 1D,E,H). In the majority of animals (5/6), removing three of the four copies of the co-receptors (*Wise*$^{-/-}$;*Lrp5*$^{-/-}$;*Lrp6*$^{+/-}$) also restored the normal tooth number, size and cusp pattern in the maxilla (Fig. 1G).

The dosage-dependent rescue by decreases in *Lrp5* and *Lrp6* demonstrates that most, if not all, of the diverse tooth defects of *Wise*-null mice are mediated by Lrp5/6-dependent processes. Although these experiments show that the Wnt co-receptors have overlapping and additive roles in tooth development, they also illustrate that the individual *Lrp5* and *Lrp6* genes contribute differently to regional aspects of tooth development. To probe this issue, we examined the expression pattern of *Lrp5* by in situ hybridization and of *Lrp6* by detection of *LacZ* expression from the *Lrp6*-null allele. We found that both genes are broadly expressed in dental epithelium and mesenchyme (data not shown). Hence, differential patterns of expression do not appear to account for specific roles for each co-receptor in tooth development. With respect to Wnt ligands, expression analyses have showed that multiple Wnt ligands are differentially expressed in early tooth germs (Sarkar and Sharpe, 1999).

Elevated Wnt signaling leads to continuous development of R2

The dependence of the *Wise* phenotypes on *Lrp5* and *Lrp6* suggests that elevated Wnt signaling in the absence of *Wise* causes the tooth abnormalities both in incisors and molars. Previously, Munne et al. reported an additional epithelial Wnt activity in *Wise*-null incisors utilizing the *Top-Gal* transgenic line (DasGupta and Fuchs, 1999; Munne et al., 2009). To monitor Wnt signaling during molar development, we also used the *Top-Gal* reporter and observed dynamic changes in the relative levels, number and spatial distribution of sites of *Top-Gal* expression during early stages of tooth development (E12.5-E15.5) in *Wise* mutants (Fig. 2A-H). Therefore, we investigated how these early alterations in Wnt activity might account for tooth abnormalities observed in adult *Wise*-null mice.

In mouse tooth development, premolars do not form, contributing to a toothless diastema region between the incisors and molars (Fig. 3A). Tooth buds are initiated in the diastema but they regress (Peterkova et al., 2006; Viriot et al., 2000). Two diastema buds, called ‘MS’ and ‘R2’ for historical reasons, form in a progressive anterior-posterior (AP) manner (Fig. 3A). MS is the first to form (E12.5), followed by R2 in the adjacent posterior territory (E13.5). At E14.5, as MS and R2 continue to regress, the first molar (M_1) begins to develop posterior to R2. The lack of markers for such transient structures has made it difficult to follow the fate of the diastema buds.

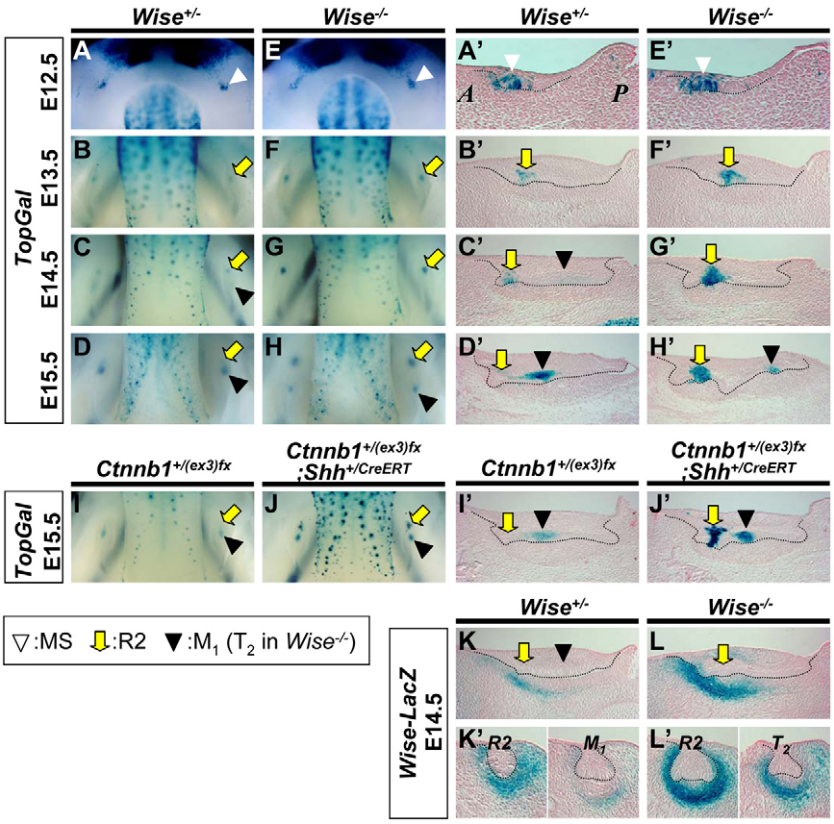

Fig. 2. Elevated Wnt signaling and continuous development of the R2 vestigial bud. (**A-H**) Wholemount *Top-Gal* expression in tooth germs of E12.5-E15.5 mandibles. (**A′-H′**) Parasagittal sections (anterior to the left) of the tooth germs from panels A-H show *Top-Gal* expression in the epithelial signaling center of the vestigial buds MS and R2, and in M_1. (**I-J′**) Tamoxifen (Tmx)-inducible mutation of β-catenin leads to ectopic Wnt activation in *Shh*-expressing cells of R2 and M_1 and continued development of R2. Tmx was injected at E13.5. (**K-L′**) *Wise-LacZ* BAC reporter expression in E14.5 tooth germs. Parasagittal (K,L) and frontal (K′,L′) sections showing reporter expression in mesenchymal cells. The dotted lines indicate the boundary between the dental epithelium and mesenchyme.

We generated parasagittal sections to precisely map the domains of reporter staining (Fig. 2A′-H′). *Top-Gal* expression is colocalized with the markers of the epithelial signaling center in early tooth buds as well as the enamel knot of the cap stage molars (Fig. 2; see Fig. S2 in the supplementary material). In control mice, the MS and R2 vestigial buds were marked by *Top-Gal* at E12.5 and E13.5, respectively (Fig. 2A′,B′). At E14.5, *Top-Gal* staining was maintained in R2 and a new domain appeared in M_1 (Fig. 2C′). By E15.5, reporter staining in R2 was almost undetectable, whereas it significantly increased and expanded in M_1 (Fig. 2D′). The transient *Top-Gal* expression in MS and R2 is consistent with the regression of these vestigial buds (Fig. 3A).

In *Wise*-null mandibles, *Top-Gal* expression was slightly increased in MS at E12.5 (Fig. 2E′). We detected elevated and sustained reporter staining in R2 from E13.5-E15.5 (Fig. 2F′-H′). R2 displayed characteristics of an advanced cap stage tooth germ at E14.5, suggesting that it continued to develop rather than regress. Reporter staining in the mutant M_1 region was delayed by one day, being first detected at E15.5 (Fig. 2H′).

To determine whether activation of Wnt signaling is sufficient for survival of R2, we genetically elevated Wnt signaling utilizing a conditional gain-of-function allele (*Ctnnb1*$^{(ex3)fx}$) of the β-*catenin* gene (Harada et al., 1999). By combining it with a Tamoxifen-inducible *Shh*^{CreERT} allele (Hayashi and McMahon, 2002), Wnt signaling was activated in the *Shh*-expressing cells of R2 and M_1 as shown by elevated *Top-Gal* expression (Fig. 2I-J′). Sustained Wnt activation led to continuous development of R2, as evidenced by invagination and morphogenesis (Fig. 2J′). These data underscore the crucial role of Wnt signaling in determining the fate of R2.

A previous study on the root pattern of maxillary molars suggested that the large molar of *Wise*-null mice was formed by fusion of multiple molars (Ohazama et al., 2008). To further explore the impact of sustained growth of R2 in *Wise*-null mice, the root pattern of the mandible was examined. In wild-type mandibles, each quadrant contains five roots: the first and second roots in M_1, the third and fourth roots in M_2 and the fifth root in M_3 (Fig. 3B). The same total number of roots was observed in *Wise*-null and *Wise*$^{-/-}$;*Lrp5*$^{-/-}$ mice (Fig. 3C,D). However, in both mutants, T_1 only contained a single enlarged root and T_2 contained the second and third roots, although the second and third roots were often fused in *Wise*-null mice. T_3 and T_4 each had a single root. These changes demonstrated that the tooth field was repartitioned in the mutants as a consequence of the survival of R2.

The temporal changes in Wnt signaling together with alterations in the root pattern suggest that, in *Wise* mutants, R2 overcame developmental arrest and continued to grow, eventually forming T_1. Correlated with these changes in R2, M_1 displayed delayed development and subsequently gave rise to the second tooth (T_2; Fig. 3A).

Wise expression in tooth development

To monitor *Wise* expression during tooth development, we generated transgenic mice harboring a *Wise-LacZ* BAC reporter construct. The *Wise-LacZ* expression mimicked endogenous gene expression in the tooth germ (Fig. 2K; see Fig. S3D,E in the supplementary material) (Laurikkala et al., 2003). At E12.5, *Wise* expression was dynamic and appeared in the epithelium immediately surrounding the signaling center and in the underlying mesenchyme of MS (see Fig. S2D′ in the supplementary material). At E14.5, the *Wise-LacZ* reporter was strongly expressed in the condensing mesenchymal cells adjacent to R2 (Fig. 2K,K′). Weaker expression was also detected in the outermost layer of mesenchymal cells in the M_1 region (Fig. 2K′). *Wise-LacZ* reporter expression was strongly upregulated in the developing R2 region of *Wise*-null tooth germ (Fig. 2L,L′), suggesting the presence of a negative-feedback loop.

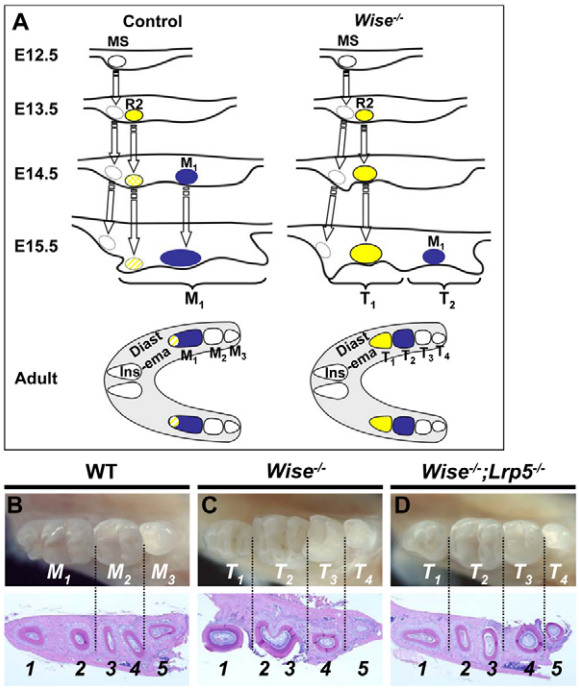

Fig. 3. Abnormal partitioning of the tooth field in *Wise*-null mice. (**A**) Schematic diagrams summarizing the fate of tooth buds in control and *Wise*-null mice. (**B-D**) The root pattern indicates that the tooth field was repartitioned in *Wise*-null mice. Mandibular molars (top) and corresponding coronal sections (bottom).

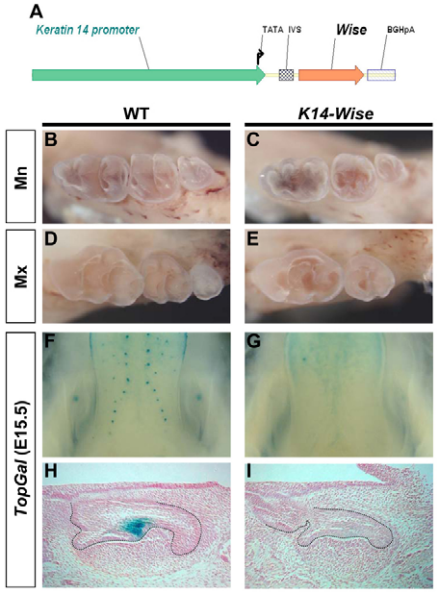

Fig. 4. Overexpression of *Wise* disrupted tooth development. (**A**) *K14-Wise* transgene. (**B-E**) Molars of transgenic mice were smaller with an abnormal cusp pattern and M_3 was frequently missing in the maxilla (E). (**F-I**) In the *K14-Wise;Top-Gal* embryo, tooth germs were growth-retarded with reduced *Top-Gal* expression, as shown in wholemount lower jaws (F,G) and frontal sections (H,I). Mn, mandibular; Mx, maxillary.

Overexpression of *Wise* disrupts tooth development

We used gain-of-function to investigate the inhibitory potential of Wise on the Wnt pathway in tooth development. Transgenic mice overexpressing *Wise* in epidermal tissues using the human keratin 14 promoter (*K14-Wise*) displayed a variety of tooth abnormalities including reduced size, loss of M_3 in the maxilla and cusp defects (Fig. 4A-E). To determine how Wnt signaling is affected by *Wise* overexpression, we also monitored *Top-Gal* expression in *K14-Wise* transgenic embryos. We found that tooth germs were growth-retarded and displayed reduced levels of *Top-Gal* expression (Fig. 4F-I). The data indicate that ectopic Wise can disrupt tooth development by inhibiting Wnt signaling.

Sustained proliferation and survival of the R2 bud in the *Wise*-null mice

The loss of *Wise* resulted in elevated epithelial Wnt activity, which promoted the continuous development of R2. To investigate the basis of altered R2 development, we examined rates of cell proliferation and cell death (Fig. 5A-H). BrdU incorporation assays showed that the non-proliferating epithelial signaling center of R2 was surrounded by proliferating epithelial and mesenchymal cells in both control and *Wise*-null embryos at E13.5 (Fig. 5A,B). No obvious differences were observed between control and *Wise*-null tooth germs at this stage. However, in *Wise*-null tooth germs at E14.5, unlike control mice, robust proliferation was detected in the underlying mesenchyme of R2 (Fig. 5C,D, asterisk). In addition, the non-proliferating epithelial signaling center of R2 was maintained only in the mutants. At this stage, a new epithelial signaling center (M_1) emerged posterior to R2 in control mice, but evidence for initiation of M_1 was not observed in the posterior region of *Wise*-null mice, providing further evidence for delayed development of M_1 (Fig. 5C,D).

To examine the rate of cell death, cells undergoing apoptosis were labeled by immunostaining against activated caspase 3 (Shigemura et al., 2001). A small group of apoptotic cells marked the primary enamel knot from E14.5-E15.5, but no significant difference was observed between control and mutant tooth germs over these stages (Fig. 5E-H). This indicated that apoptosis was unlikely to play a crucial role in determining the fate of R2. This is in agreement with recent genetic studies that suggested apoptosis is largely dispensable for tooth development (Matalova et al., 2006; Setkova et al., 2007).

The fate and contribution of cells from MS and R2 to M_1 has been difficult to determine because these structures are normally transient in nature and undergo degeneration. We first examined the expression of *Shh*, an established enamel knot marker (Hardcastle et al., 1998). In control animals, *Shh* was progressively activated in a transient manner in MS and R2 and, by E15.5, *Shh* expression was observed only in the M_1 enamel knot of control mice (Fig. 5I,I′). By contrast, as previously shown in *Wise*-null mice (Kassai et al., 2005), *Shh* expression was sustained in R2 and also present in M_1 at E15.5 (Fig. 5J,J′). To trace the fate of cells descended from the MS and R2 in control and *Wise*-null mice, we utilized a *GFP-Cre* knock-in allele of the *Shh* gene (Harfe et al., 2004). In combination with an *R26R-floxstop-LacZ* reporter line, descendants of cells that had expressed *Shh* at earlier stages were genetically marked. At E15.5, the putative MS and R2 regions anterior to M_1 were occupied by the descendants of the *Shh*-expressing cells in control tooth germs (Fig. 5K,K′). To ensure that the large group of

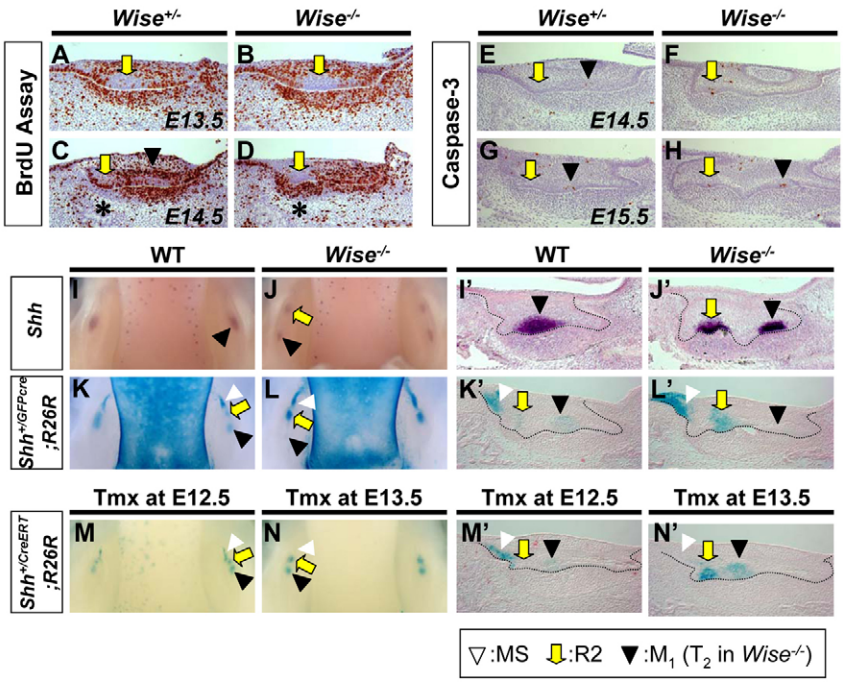

Fig. 5. Proliferation and fate-mapping of the vestigial buds. (**A-D**) BrdU incorporation assays measuring cell proliferation in tooth germs. Asterisks mark mesenchymal cells underlying R2. (**E-H**) Immunostaining for cleaved caspase 3 to detect apoptotic cells. (**I-J′**) *Shh* was ectopically expressed in R2 of *Wise*-null tooth germs at E15.5, as shown in the whole mandibles (I,J) and on parasagittal sections (I′,J′). (**K-L′**) *Shh*-expressing cells and their descendants were marked by β-gal staining of the $Shh^{+/GFPcre}$;*R26R* embryos at E15.5. (**M-N′**) Tmx-induced labeling of the descendants of *Shh*-expressing cells indicates that MS contributes to the anterior outer enamel epithelium of M_1.

positive cells anterior to R2 were actually descended from MS and not from cells present in other, earlier domains of *Shh* expression, we utilized the Tamoxifen-inducible Shh^{CreERT} allele to mark cells at a specific stage. By comparing *LacZ*-positive cells after Tamoxifen injection at E12.5 and E13.5, we confirmed that descendants of MS contribute to the dental epithelial cells anterior to R2 at E15.5 (Fig. 5M-N′). Staining in both the MS and R2 regions was greatly expanded in *Wise*-null tooth germs (Fig. 5L,L′). This was consistent with continued expression of *Shh* in R2 at earlier stages and underscored the fact that MS was also altered in the mutant (see Figs S2, S3 in the supplementary material).

Fgf and Shh pathways are major targets of Wise-regulated Wnt signaling

Our analyses demonstrate that inactivation of *Wise* leads to increased signaling activity in R2 as early as E13.5, whereas the morphological differences only become apparent a day later. To examine the degree to which signaling pathways were misregulated in the R2 of *Wise*-null mice, tooth germs were dissected from E13.5 mandibles and expression analysis was performed using qPCR arrays designed for Wnt, Tgfβ and/or Bmp, hedgehog and growth factor pathways (SABiosciences). Differential expression was confirmed for some of the genes by wholemount in situ hybridization (see Fig. S3 in the supplementary material). Major changes were observed in components of the Fgf and Shh pathways with a large increase in several Fgf genes and *Shh* (Table 1), whereas some minor alterations were observed in Tgfβ and/or Bmp or other pathways (see Table S1 in the supplementary material).

Genetic interaction between *Wise* and *Shh*

The significant changes in gene expression observed for several components of the Shh signaling pathway and elevated *Patch1-LacZ* expression (see Fig. S3 in the supplementary material) in the *Wise*-null tooth buds prompted us to investigate genetic interactions between *Wise* and *Shh*. There were no detectable tooth phenotypes in the $Shh^{+/GFPcre}$ or $Wise^{+/-}$ heterozygous mice (Fig. 6A). Hence, we were surprised to discover that a supernumerary tooth anterior to M_1 was generated in $Wise^{+/-}$;$Shh^{+/GFPcre}$ mice with high penetrance (81%, n=42; Fig. 6B). The Shh^{GFPcre} allele displayed a dynamic pattern of *Gfp* expression in the diastema buds and molars that mimicked expression of the endogenous *Shh* gene (Fig. 6D-L). The tooth phenotype in double-heterozygous embryos correlated with changes in the temporal pattern of *Shh* as *Gfp* expression was significantly elevated in R2 and restricted to a smaller domain of cells in M_1 at E14.5 (Fig. 6H). At E15.5, double-heterozygous embryos continued to express *Gfp* in R2 and expression in the M_1 enamel knot appeared to be smaller and shifted posteriorly (Fig. 6K). These results indicate that, in the compound heterozygous mutants, R2 escaped developmental arrest to form a cap-stage tooth and initiation and/or growth of M_1 was delayed. Two additional *Shh*-null alleles, Shh^{creERT} and Shh^{neo}, also generated the same

Table 1. Differentially expressed genes in *Wise*-null tooth germs at E13.5 identified in qPCR arrays

Gene	*t*-test (*P*-value)	Fold upregulation or downregulation (Mut/Het)
Dkk1	0.0004	2.55
Wnt7a	0.0042	–2.67
Foxn1	0.0253	–1.88
Lef1	0.0096	1.23
Fgf3	0.0000	9.19
Fgf4	0.0000	9.70
Fgf15	0.0194	4.10
Fgfr1	0.0243	1.68
Pea3	0.0042	2.31
Spry2	0.0130	1.50
Spp1	0.0192	–1.92
Shh	0.0156	3.32
Ptch1	0.1202	1.56
Ptch2	0.0427	1.73
Ptchd2	0.0149	2.03
Erbb4	0.0023	–1.70
p21	0.0076	1.74
Dlx2	0.0157	1.46

Genes with >1.4-fold change ($P \leq 0.05$) are shown.

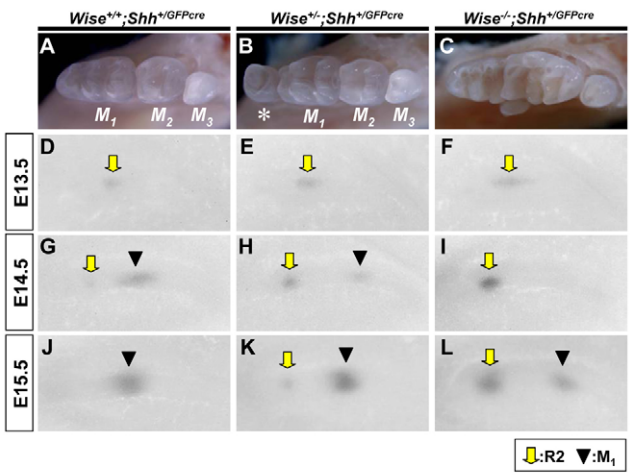

M

	T_1-T_2 fusion (%)	T_2-T_3 fusion (%)	Lateral tooth (%)
Wise$^{-/-}$ (n=16)	50.0	37.5	56.3
Wise$^{-/-}$;*Shh*$^{+/-}$ (n=18)	100	94.4	88.9

N

	Wise$^{+/-}$;*Shh*$^{+/-}$	*Wise*$^{+/-}$;*Shh*$^{+/-}$;*Ptch1*$^{+/-}$	*Wise*$^{+/-}$;*Shh*$^{+/-}$;*Lrp6*$^{+/-}$
Supernumerary tooth (%)	81.0 (n=42)	33.3 (n=18)	9.1 (n=22)

Fig. 6. Genetic interaction between *Wise*, *Shh*, *Ptch1* and *Lrp6*. (**A-C**) Adult molars in the mandible. The asterisk marks a supernumerary tooth. (**D-L**) *Gfp* expression from the *GfpCre* knock-in *Shh* allele in wholemount tooth germs shown as inverted gray scale. (**M**) Exacerbation of *Wise*-null tooth phenotypes by reducing *Shh* dosage. (**N**) Rescue of *Wise*$^{+/-}$;*Shh*$^{+/-}$ supernumerary tooth by reducing dosage of *Ptch1* or *Lrp6*. The *Shh*^{GFPcre} allele in a C57/BL6 background was used for analyses. *n*, number of mandibular jaw quadrants.

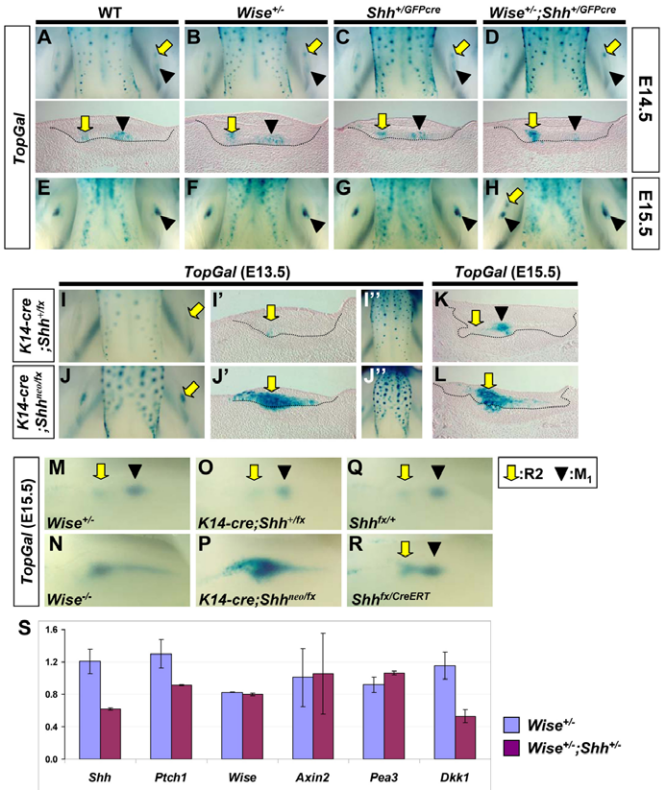

Fig. 7. *Shh* negatively regulates Wnt signaling in tooth germs. (**A-H**) Wnt signaling was elevated in R2 of *Wise*$^{+/-}$;*Shh*$^{+/-}$ mice, as shown by *Top-Gal* expression in whole mandibles and parasagittal sections. (**I-L**) *Top-Gal* expression was elevated in *Shh*-deficient (*K14-cre;Shh*$^{neo/fx}$) tooth germs. Increased *Top-Gal* expression was also observed in fungiform taste papillae (I″,J″). (**M-R**) *Top-Gal* expression in the maxillary tooth germs of *Wise* (M,N), *K14-cre;Shh*$^{neo/fx}$ (O,P) and *Shh*$^{fx/CreERT}$ (Q,R; Tmx injection at E13.5) mice. (**S**) qPCR analysis of selected genes in *Wise*$^{+/-}$ and *Wise*$^{+/-}$;*Shh*$^{+/-}$ tooth germs at E13.5.

supernumerary tooth phenotype when combined with the *Wise* mutant allele (data not shown). A reduction in the dosage of *Shh* significantly increased the severity of *Wise*-null molar phenotypes (Fig. 6C,M). *Gfp* expression in the *Wise*$^{-/-}$;*Shh*$^{+/GFPcre}$ tooth germs was elevated to even higher levels in R2, and it was more delayed in M_1 (Fig. 6I,L).

These genetic interactions demonstrated that phenotypes in *Wise* mutant backgrounds were highly sensitive to the dosage of *Shh* and thus presumably to levels of Shh signaling. Therefore, we tested the effect of reducing *Ptch1*, which encodes a negative regulator of Shh signaling. Removal of one copy of *Ptch1* significantly decreased the frequency of the supernumerary tooth phenotype in *Wise*$^{+/-}$;*Shh*$^{+/GFPcre}$ mice (33%, n=18, P<0.0002; Fig. 6N). This suggests that reduced Shh signaling was the cause of the defect in *Wise*$^{+/-}$;*Shh*$^{+/GFPcre}$ mice.

Shh negatively regulates Wnt signaling in tooth germs

The effects seen upon reduction of *Shh* might reflect changes in Wnt signaling. Therefore, we measured *Top-Gal* activity in tooth germs with varying dosages of *Wise* and *Shh* (Fig. 7A-D). There was no change in patterns of reporter expression in *Wise*$^{+/-}$ or *Shh*$^{+/GFPcre}$ mice compared with control animals. However, in the *Wise*$^{+/-}$;*Shh*$^{+/GFPcre}$ tooth germs, *Top-Gal* expression was significantly increased in R2 and delayed in M_1 (Fig. 7D). Furthermore, reducing the dosage of *Lrp6* rescued the supernumerary tooth formation in the majority of *Wise*$^{+/-}$;*Shh*$^{+/GFPcre}$;*Lrp6*$^{+/-}$ mice (20/22; Fig. 6N). The elevated Wnt signaling and genetic rescue by *Lrp6*$^{+/-}$ in the compound mutants closely resemble those observed in *Wise*-null mice, suggesting that the reduction in Shh signaling leads to sustained growth of R2 through an elevation in Wnt signaling.

These genetic data point to a role for Shh as an antagonist of Wnt signaling and a suppressor of the bud-to-cap transition of R2. In addition, enhanced tooth fusion in *Wise*$^{-/-}$;*Shh*$^{+/-}$ mice implies that Shh is required for separation of teeth by antagonizing Wnt signaling as the fusion phenotype was highly sensitive to dosage of *Lrp5*. To investigate this idea, we have utilized a conditional allele of *Shh* (*Shh*^{fx}) in combination with a *K14-Cre* driver to delete *Shh* in the dental epithelium. In the *K14-Cre;Shh*$^{neo/fx}$ mice, *Top-Gal* expression in tooth germs was highly upregulated compared with control mice (Fig. 7I-L,I′,J′). Elevation of Wnt signaling was also observed in the maxilla where a single extended domain of *Top-Gal* expression was associated with tooth fusion (Fig. 7M-P). To rule out the possibility that the elevated Wnt signaling is an indirect effect of disruption in earlier tooth development, *Shh* was

temporally reduced in R2 and M_1 buds using the *Shh*^{CreERT} allele. Two days after Tamoxifen injection, *Top-Gal* was upregulated in the tooth buds, which appeared to be fused (Fig. 7Q,R). These data support the idea that Shh suppresses the survival of R2 and prevents fusion between neighboring teeth by antagonizing Wnt signaling. We also observed elevated levels of *Top-Gal* staining in taste papillae and hair follicles in these conditional *Shh* mutants (Fig. 7I″,J″; data not shown). Therefore, Shh might have a related role in modulating Wnt signaling in other tissue contexts (Iwatsuki et al., 2007).

To identify candidate genes that might participate in the antagonistic action of Shh on Wnt signaling, we utilized qPCR to examine the expression of 90 selected genes relevant to tooth development, including the differentially regulated genes in *Wise*-null tooth germs (Table 1). Besides *Shh*, *Dkk1* was downregulated by about 50% in *Wise*$^{+/–}$;*Shh*$^{+/–}$ tooth germs at E13.5 compared with *Wise*$^{+/–}$ tooth germs (Fig. 7S). *Dkk1* was the only gene that showed more than 1.6-fold change (P<0.05), suggesting that it is an early downstream target of Shh (data now shown). This raises the possibility that simultaneous reduction of the two Wnt antagonists, Wise and Dkk1, might account for the elevation of Wnt signaling above a threshold level and lead to survival of R2 in *Wise*$^{+/–}$;*Shh*$^{+/–}$ mice.

DISCUSSION

In this study, we have demonstrated that precise control of the level of Wnt signaling plays a crucial role in determining whether diastema buds survive and go on to develop into mature teeth. We have also shown that survival of a diastema bud results in delayed development of the adjacent posterior molar buds, suggesting that reduced inhibitory signals resulting from the regression of R2 might be a prerequisite for the timely initiation of M_1. These tissue interactions between developing buds are consistent with a temporal model for tooth formation in which pre-existing tooth buds inhibit initiation of new posterior teeth and form a progressive inhibitory cascade affecting the timing of tooth formation (Kavanagh et al., 2007). We have shown that, in tooth development, Wise suppresses survival of the diastema and incisor vestigial buds by serving as an inhibitor of Lrp5- and Lrp6-dependent Wnt signaling. Our genetic and expression analyses reveal that the Fgf and Shh pathways are major downstream targets of the Wnt signaling regulated by Wise. Furthermore, through genetic interaction studies, we have discovered that Shh acts as a negative-feedback regulator of Wnt signaling during the bud-to-cap transition. Our data provide insight into the mechanisms that control the levels of Wnt signaling and crosstalk between the Wnt, Shh and Fgf pathways that regulate the timing and number of teeth.

Wise as a Wnt antagonist

In *Wise* mutants, our qPCR array data indicated that expression of Wnt pathway components was only moderately affected and the Wnt pathway activity as a whole was highly elevated, as detected by *Top-Gal*. Conversely, overexpression of *Wise* resulted in reduced Wnt activity in the dental epithelium and inhibition of tooth growth. The phenotypes of our *K14-Wise* mice (Fig. 4; data not shown) were also strikingly similar to those of *K14-Dkk1* mice, with abnormal development of multiple tissues including hair follicles, mammary glands, taste buds and teeth (Andl et al., 2002; Chu et al., 2004; Liu et al., 2008). The upregulation of *Wise-LacZ* reporter expression in *Wise*-null tooth germs implies that *Wise* might be activated by signaling molecules from the enamel knot through a negative-feedback loop. This is consistent with the elevated *Wise* expression observed in tooth germs with constitutively active Wnt signaling (Jarvinen et al., 2006; Liu et al., 2008).

The genetic interaction data revealed that, in the absence of *Wise*, multiple aspects of abnormal tooth development are highly sensitive to the dosage of *Lrp5* and *Lrp6*. Complete rescue of the *Wise*-null molar and incisor phenotypes was only observed in *Lrp5*$^{–/–}$;*Lrp6*$^{+/–}$ mice, indicating that both genes contribute to Wnt signaling in tooth development. This supports a model whereby Wise acts as a Wnt antagonist through its direct interaction with these Wnt co-receptors. In the absence of inhibition by Wise, there is an elevation of Lrp5/6-dependent Wnt signaling, which induces tooth phenotypes. Decreasing copies of the Lrp5/6 co-receptors rescues the *Wise*-null phenotypes presumably through restoration of normal levels of Wnt activity. There were no obvious tooth abnormalities in *Lrp5*$^{–/–}$;*Lrp6*$^{+/–}$ mice in the presence of *Wise*. This indicates that one copy of *Lrp6* is sufficient to provide levels of Wnt signaling able to potentiate normal tooth development. This could be a consequence of feedback mechanisms that would compensate for reduced levels of the co-receptor (Fig. 8).

Lrp4 might provide an additional means through which Wise mediates antagonistic action on Wnt signaling. Lrp4 can antagonize canonical Wnt signaling when overexpressed in cultured cells (Li et al., 2010). Although in vitro Wise can bind to Lrp4 (Ohazama et al., 2008), it is unknown whether interactions with Wise can influence Lrp4 function. Developmental abnormalities associated with inactivation of *Lrp4* were similar to Wnt loss-of-function phenotypes in certain tissues rather than phenotypes caused by excess Wnt signaling (Choi et al., 2009; Weatherbee et al., 2006). This suggests that the function of Lrp4 can be context-dependent. As mice homozygous for a hypomorphic allele of *Lrp4* displayed tooth defects similar to those of *Wise*-null mice, it was proposed that Wise binds to Lrp4 to initiate intracellular events leading to inhibition of Wnt signaling (Ohazama et al., 2008). Overgrowth and fusion of molars in these *Lrp4* mutant mice was associated with elevated Wnt signaling, as assayed by BAT-gal staining in bell-stage tooth germs (Ohazama et al., 2008), but the early changes in Wnt, Shh and other signaling activities have not been examined in *Lrp4* mutant mice. Preliminary analyses of mice homozygous for a null allele of *Lrp4* (Weatherbee et al., 2006) have shown that loss of *Lrp4* does not phenocopy loss of *Wise* during R2 development. This raises the possibility that Lrp4 and Wise play distinct roles in the diastema buds and that multiple molecular mechanisms underlie tooth defects in these two mouse mutant models.

Signaling network in diastema tooth development

In the diastema region of the mouse, it has been proposed that phylogenetic memory of odontogenesis is manifested by the formation of vestigial tooth buds that undergo degeneration without reaching the cap stage. In mouse models with genetic disruptions of major signaling pathways, a supernumerary tooth forms in front of M_1, indicating that crosstalk between many pathways is involved in controlling diastema tooth development. In this regard, our analyses with *Wise* mutants have shed light on the important role of Wnt signaling in these events.

Data with the *Top-Gal* reporter in control and *Wise*-null mice demonstrated that Wnt signaling is sequentially activated in epithelia of the two vestigial buds, MS and R2, and then subsequently in molar buds M_1, M_2 and M_3. However, during normal development, *Top-Gal* expression is rapidly downregulated

in MS and R2 in contrast to the M_1-M_3 buds, coincident with the inability of the rudimentary buds to make the bud-to-cap transition. Reporter analysis showed that *Wise* is highly expressed in the mesenchymal cells that surround the arrested buds. The loss of *Wise* leads to elevated and sustained levels of Wnt signaling in the epithelium and continuous development of R2.

Together with the fate mapping data that shows the persistence of descendants of *Shh*-positive cells, the results from cell proliferation and cell death analyses suggest that the transition is controlled largely by proliferative signals from the epithelial signaling center to the surrounding mesenchyme. Fgf4 is a strong candidate for the signals, as it is an epithelial target of Wnt signaling and can rescue the developmental arrest of cultured *Lef1* mutant tooth germs with its ability to activate mesenchymal *Fgf3* expression (Kratochwil et al., 2002). Our quantitative expression analyses showed that *Fgf4*, as well as *Fgf3*, are highly upregulated in *Wise*-null tooth germs, further supporting the notion that Fgf signaling is a major downstream target of epithelial Wnt signaling.

There are similarities and differences in the roles for Wise in molar and incisor development. In both molars (Fig. 2) and incisors (Munne et al., 2009), Wnt signaling is significantly elevated, in agreement with the idea that Wise can inhibit the Wnt pathway. Furthermore, reducing the dosage of the Lrp co-receptors rescues supernumerary tooth phenotypes in molars and incisors (Fig. 1). With respect to cell death in R2 and incisors, there were a limited number of apoptotic cells at early stages (Fig. 5) (Munne et al., 2009). However, reduction in the number of apoptotic cells was reported in later stage incisors (Munne et al., 2009; Murashima-Suginami et al., 2007), suggesting that apoptosis might play a different role in incisors compared with molars.

Interaction between *Shh* and Wnt signaling in diastema tooth development

An important aspect of the regulatory network uncovered by our studies was the nature of the genetic interactions between *Wise* (Wnt signaling) and *Shh* in tooth development. In normal tooth development, there was a tight spatial and temporal correlation between Wnt activity and *Shh* expression in the epithelial signaling center of tooth buds. The elevated Wnt signaling in *Wise*-null mice led to increased *Shh* expression in the R2 bud. Ectopic activation of Wnt signaling in the dental epithelium has been shown to induce Shh expression in tooth buds (Jarvinen et al., 2006; Wang et al., 2009). Inactivation of Wnt signaling results in loss of *Shh* expression (Liu et al., 2008). These data indicate that the level of *Shh* expression in the developing tooth bud is dependent upon the relative level of Wnt signaling. Conversely, we have found that Shh modulates levels of Wnt signaling. In $Wise^{+/-};Shh^{+/-}$ mice, Wnt signaling was significantly elevated, leading to survival of R2 and supernumerary tooth formation. This suggests that Shh signaling normally participates in a negative-feedback loop that controls the level of Wnt signaling in R2 (Fig. 8).

A key aspect of this regulatory model is that maintaining a proper balance between Wnt and Shh signaling is more important than the absolute level of either signaling activity. For example, during normal development of R2, levels of Wnt signaling are relatively low and transient. Therefore, low levels of Shh are sufficient to repress Wnt activity and suppress the bud-to-cap transition of R2. Phenotypes arise when either of the pathways is disrupted and normal regulatory feedback modulations are unable to restore a proper balance at the appropriate time. Fig. 8 presents a model for the regulatory interactions between signaling components in R2 of wild-type and genetic mutant backgrounds.

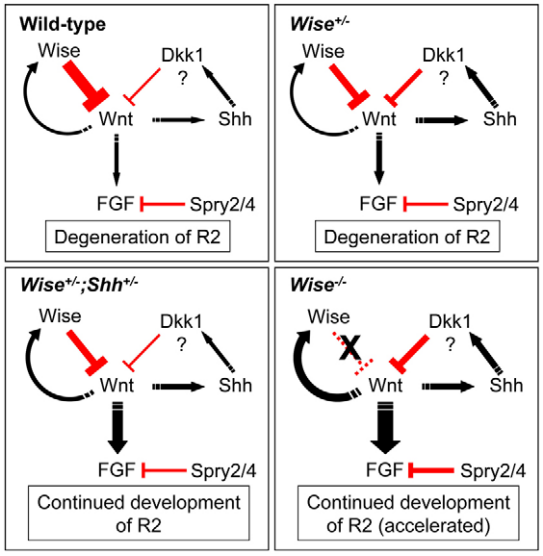

Fig. 8. Model for signaling network in diastema tooth development. Schematic diagrams of the signaling network regulating development of the diastema R2 bud at E13.5-E14.5 in wild-type and genetic mutant backgrounds. In wild-type teeth, Wnt signaling is required for the bud-to-cap transition of R2 by inducing Fgfs. Wise and Spry2/4 antagonize Wnt and Fgf signaling, respectively, to suppress the transition. Shh is a downstream target of Wnt signaling and acts as a negative-feedback regulator of Wnt signaling via *Dkk1* and other targets. Elevated Wnt signaling feeds back to stimulate Wise expression. The thickness of the lines represents relative levels of activity. Red indicates repressive input and black indicates positive input to activity.

This hypothesis was further supported by the observation that reducing the dosage of *Ptch1* (elevating Shh signaling) or *Lrp6* (reducing Wnt signaling) rescues the supernumerary tooth phenotype of $Wise^{+/-};Shh^{+/-}$ mice. We also observed elevated Wnt signaling in *Shh*-deficient tooth buds. This inhibitory role of Shh on Wnt signaling in the bud-to-cap transition is consistent with the recent finding that ectopic Shh activity in *K14-Shh* mice arrests tooth development at the bud stage (Cobourne et al., 2009). In addition to the early role in R2, Shh signaling is required for proper separation of teeth (Gritli-Linde et al., 2002; Ohazama et al., 2008), consistent with the exacerbated fusion in $Wise^{-/-};Shh^{+/-}$ mice. The elevated Wnt signaling in the *Shh*-deficient tooth germs suggests that Shh prevents tooth fusion by antagonizing Wnt signaling.

Recently, ectopic tooth formation was reported in mice deficient for polaris and *Gas1* (Ohazama et al., 2009). Polaris is a component of primary cilia which is required for Shh signaling (Huangfu et al., 2003). Gas1 acts as a facilitator of Shh signaling in different developmental contexts (Allen et al., 2007; Martinelli and Fan, 2007; Seppala et al., 2007). Our genetic data on interactions between Shh and Wnt signaling suggest that the supernumerary tooth in polaris and *Gas1* mutant mice results from disruption of the Wnt-Shh feedback loop in R2, in which temporal reduction in Shh signaling results in elevated Wnt signaling and hence survival of R2.

In conclusion, our findings highlight how the processes of tooth development are highly sensitive to spatiotemporal changes in Wnt signaling activity. Even a small disruption in the signaling network, through loss or gain of Wnt antagonists (Wise) or feedback regulators such as Shh, is sufficient to change the fate of tooth buds, leading to abnormal tooth number and size. Changes in

expression of signaling modulators such as Wise might represent an important mechanism that underlies the evolutionary diversity in mammalian dentition.

Acknowledgements
We thank S. Miura for analysis of the Bmp pathway, G. R. Martin for discussion and providing the *Fgf10*, *Fgfr1* and *Fgfr2* mutants and the following for providing mutant mouse lines: L. Chan, *Lrp5*; W. C. Skarnes, *Lrp6*; M. Taketo, *Ctnnb1*$^{(ex3)fx}$; C. Tabin and B. Harfe, *Shh*^{GFPcre} and *Shh*^{creERT}; P. Beachy, *Shh*^{neo}; A. P. McMahon, *Shh*^{fx}; M. P. Scott, *Ptch1*^{LacZ}; and Y. Mishina, *Bmpr1a*. We thank M. L. Johnson, D. L. Ellies and Krumlauf laboratory members for discussions, the Stowers Institute histology facility, K. Westpfahl for animal support and S. D. Weatherbee for sharing unpublished data on *Lrp4* mutants. Y.A., B.W.S. and R.K. were supported by funds from the Stowers Institute.

Competing interests statement
The authors declare no competing financial interests.

Supplementary material
Supplementary material for this article is available at
http://dev.biologists.org/lookup/suppl/doi:10.1242/dev.054668/-/DC1

References

Allen, B. L., Tenzen, T. and McMahon, A. P. (2007). The Hedgehog-binding proteins Gas1 and Cdo cooperate to positively regulate Shh signaling during mouse development. *Genes Dev.* **21**, 1244-1257.
Andl, T., Reddy, S. T., Gaddapara, T. and Millar, S. E. (2002). WNT signals are required for the initiation of hair follicle development. *Dev. Cell* **2**, 643-653.
Chiang, C., Litingtung, Y., Lee, E., Young, K. E., Corden, J. L., Westphal, H. and Beachy, P. A. (1996). Cyclopia and defective axial patterning in mice lacking Sonic hedgehog gene function. *Nature* **383**, 407-413.
Choi, H. Y., Dieckmann, M., Herz, J. and Niemeier, A. (2009). Lrp4, a novel receptor for Dickkopf 1 and sclerostin, is expressed by osteoblasts and regulates bone growth and turnover in vivo. *PLoS ONE* **4**, e7930.
Chu, E. Y., Hens, J., Andl, T., Kairo, A., Yamaguchi, T. P., Brisken, C., Glick, A., Wysolmerski, J. J. and Millar, S. E. (2004). Canonical WNT signaling promotes mammary placode development and is essential for initiation of mammary gland morphogenesis. *Development* **131**, 4819-4829.
Cobourne, M. T., Xavier, G. M., Depew, M., Hagan, L., Sealby, J., Webster, Z. and Sharpe, P. T. (2009). Sonic hedgehog signalling inhibits palatogenesis and arrests tooth development in a mouse model of the nevoid basal cell carcinoma syndrome. *Dev. Biol.* **331**, 38-49.
DasGupta, R. and Fuchs, E. (1999). Multiple roles for activated LEF/TCF transcription complexes during hair follicle development and differentiation. *Development* **126**, 4557-4568.
Dassule, H. R., Lewis, P., Bei, M., Maas, R. and McMahon, A. P. (2000). Sonic hedgehog regulates growth and morphogenesis of the tooth. *Development* **127**, 4775-4785.
Ellies, D. L. and Krumlauf, R. (2006). Bone formation: The nuclear matrix reloaded. *Cell* **125**, 840-842.
Gritli-Linde, A., Bei, M., Maas, R., Zhang, X. M., Linde, A. and McMahon, A. P. (2002). Shh signaling within the dental epithelium is necessary for cell proliferation, growth and polarization. *Development* **129**, 5323-5337.
Harada, N., Tamai, Y., Ishikawa, T., Sauer, B., Takaku, K., Oshima, M. and Taketo, M. M. (1999). Intestinal polyposis in mice with a dominant stable mutation of the beta-catenin gene. *EMBO J.* **18**, 5931-5942.
Hardcastle, Z., Mo, R., Hui, C. C. and Sharpe, P. T. (1998). The Shh signalling pathway in tooth development: defects in Gli2 and Gli3 mutants. *Development* **125**, 2803-2811.
Harfe, B. D., Scherz, P. J., Nissim, S., Tian, H., McMahon, A. P. and Tabin, C. J. (2004). Evidence for an expansion-based temporal Shh gradient in specifying vertebrate digit identities. *Cell* **118**, 517-528.
Hayashi, S. and McMahon, A. P. (2002). Efficient recombination in diverse tissues by a tamoxifen-inducible form of Cre: a tool for temporally regulated gene activation/inactivation in the mouse. *Dev. Biol.* **244**, 305-318.
Huangfu, D., Liu, A., Rakeman, A. S., Murcia, N. S., Niswander, L. and Anderson, K. V. (2003). Hedgehog signalling in the mouse requires intraflagellar transport proteins. *Nature* **426**, 83-87.
Itasaki, N., Jones, C. M., Mercurio, S., Rowe, A., Domingos, P. M., Smith, J. C. and Krumlauf, R. (2003). Wise, a context-dependent activator and inhibitor of Wnt signalling. *Development* **130**, 4295-4305.
Iwatsuki, K., Liu, H. X., Gronder, A., Singer, M. A., Lane, T. F., Grosschedl, R., Mistretta, C. M. and Margolskee, R. F. (2007). Wnt signaling interacts with Shh to regulate taste papilla development. *Proc. Natl. Acad. Sci. USA* **104**, 2253-2258.
Jarvinen, E., Salazar-Ciudad, I., Birchmeier, W., Taketo, M. M., Jernvall, J. and Thesleff, I. (2006). Continuous tooth generation in mouse is induced by activated epithelial Wnt/beta-catenin signaling. *Proc. Natl. Acad. Sci. USA* **103**, 18627-18632.
Kassai, Y., Munne, P., Hotta, Y., Penttila, E., Kavanagh, K., Ohbayashi, N., Takada, S., Thesleff, I., Jernvall, J. and Itoh, N. (2005). Regulation of mammalian tooth cusp patterning by ectodin. *Science* **309**, 2067-2070.
Kato, M., Patel, M. S., Levasseur, R., Lobov, I., Chang, B. H., Glass, D. A., 2nd, Hartmann, C., Li, L., Hwang, T. H., Brayton, C. F. et al. (2002). Cbfa1-independent decrease in osteoblast proliferation, osteopenia, and persistent embryonic eye vascularization in mice deficient in Lrp5, a Wnt coreceptor. *J. Cell Biol.* **157**, 303-314.
Kavanagh, K. D., Evans, A. R. and Jernvall, J. (2007). Predicting evolutionary patterns of mammalian teeth from development. *Nature* **449**, 427-432.
Klein, O. D., Minowada, G., Peterkova, R., Kangas, A., Yu, B. D., Lesot, H., Peterka, M., Jernvall, J. and Martin, G. R. (2006). Sprouty genes control diastema tooth development via bidirectional antagonism of epithelial-mesenchymal Fgf signaling. *Dev. Cell* **11**, 181-190.
Kratochwil, K., Galceran, J., Tontsch, S., Roth, W. and Grosschedl, R. (2002). Fgf4, a direct target of LEF1 and Wnt signaling, can rescue the arrest of tooth organogenesis in Lef1(–/–) mice. *Genes Dev.* **16**, 3173-3185.
Laurikkala, J., Kassai, Y., Pakkasjarvi, L., Thesleff, I. and Itoh, N. (2003). Identification of a secreted Bmp antagonist, ectodin, integrating Bmp, Fgf, and SHH signals from the tooth enamel knot. *Dev. Biol.* **264**, 91-105.
Li, X., Zhang, Y., Kang, H., Liu, W., Liu, P., Zhang, J., Harris, S. E. and Wu, D. (2005). Sclerostin binds to LRP5/6 and antagonizes canonical Wnt signaling. *J. Biol. Chem.* **280**, 19883-19887.
Li, Y., Pawlik, B., Elcioglu, N., Aglan, M., Kayserili, H., Yigit, G., Percin, F., Goodman, F., Nurnberg, G., Cenani, A. et al. (2010). LRP4 mutations alter Wnt/beta-Catenin signaling and cause limb and kidney malformations in Cenani-Lenz syndrome. *Am. J. Hum. Genet.* **86**, 696-706.
Lintern, K. B., Guidato, S., Rowe, A., Saldanha, J. W. and Itasaki, N. (2009). Characterization of wise protein and its molecular mechanism to interact with both Wnt and Bmp signals. *J. Biol. Chem.* **284**, 23159-23168.
Liu, F., Chu, E. Y., Watt, B., Zhang, Y., Gallant, N. M., Andl, T., Yang, S. H., Lu, M. M., Piccolo, S., Schmidt-Ullrich, R. et al. (2008). Wnt/beta-catenin signaling directs multiple stages of tooth morphogenesis. *Dev. Biol.* **313**, 210-224.
Martinelli, D. C. and Fan, C. M. (2007). Gas1 extends the range of Hedgehog action by facilitating its signaling. *Genes Dev.* **21**, 1231-1243.
Matalova, E., Sharpe, P. T., Lakhani, S. A., Roth, K. A., Flavell, R. A., Setkova, J., Misek, I. and Tucker, A. S. (2006). Molar tooth development in caspase-3 deficient mice. *Int. J. Dev. Biol.* **50**, 491-497.
Milenkovic, L., Goodrich, L. V., Higgins, K. M. and Scott, M. P. (1999). Mouse patched1 controls body size determination and limb patterning. *Development* **126**, 4431-4440.
Min, H., Danilenko, D. M., Scully, S. A., Bolon, B., Ring, B. D., Tarpley, J. E., DeRose, M. and Simonet, W. S. (1998). Fgf-10 is required for both limb and lung development and exhibits striking functional similarity to *Drosophila* branchless. *Genes Dev.* **12**, 3156-3161.
Mishina, Y., Hanks, M. C., Miura, S., Tallquist, M. D. and Behringer, R. R. (2002). Generation of Bmpr/Alk3 conditional knockout mice. *Genesis* **32**, 69-72.
Munne, P. M., Tummers, M., Jarvinen, E., Thesleff, I. and Jernvall, J. (2009). Tinkering with the inductive mesenchyme: Sostdc1 uncovers the role of dental mesenchyme in limiting tooth induction. *Development* **136**, 393-402.
Murashima-Suginami, A., Takahashi, K., Kawabata, T., Sakata, T., Tsukamoto, H., Sugai, M., Yanagita, M., Shimizu, A., Sakurai, T., Slavkin, H. C. et al. (2007). Rudiment incisors survive and erupt as supernumerary teeth as a result of USAG-1 abrogation. *Biochem. Biophys. Res. Commun.* **359**, 549-555.
Ohazama, A., Johnson, E. B., Ota, M. S., Choi, H. J., Porntaveetus, T., Oommen, S., Itoh, N., Eto, K., Gritli-Linde, A., Herz, J. et al. (2008). Lrp4 modulates extracellular integration of cell signaling pathways in development. *PLoS ONE* **3**, e4092.
Ohazama, A., Haycraft, C. J., Seppala, M., Blackburn, J., Ghafoor, S., Cobourne, M., Martinelli, D. C., Fan, C. M., Peterkova, R., Lesot, H. et al. (2009). Primary cilia regulate Shh activity in the control of molar tooth number. *Development* **136**, 897-903.
Peterkova, R., Lesot, H. and Peterka, M. (2006). Phylogenetic memory of developing mammalian dentition. *J. Exp. Zool. B Mol. Dev. Evol.* **306**, 234-250.
Peterkova, R., Churava, S., Lesot, H., Rothova, M., Prochazka, J., Peterka, M. and Klein, O. D. (2009). Revitalization of a diastemal tooth primordium in Spry2 null mice results from increased proliferation and decreased apoptosis. *J. Exp. Zool. B Mol. Dev. Evol.* **312B**, 292-308.
Pinson, K. I., Brennan, J., Monkley, S., Avery, B. J. and Skarnes, W. C. (2000). An LDL-receptor-related protein mediates Wnt signalling in mice. *Nature* **407**, 535-538.
Sarkar, L. and Sharpe, P. T. (1999). Expression of Wnt signalling pathway genes during tooth development. *Mech. Dev.* **85**, 197-200.
Semenov, M., Tamai, K. and He, X. (2005). SOST is a ligand for LRP5/LRP6 and a Wnt signaling inhibitor. *J. Biol. Chem.* **280**, 26770-26775.

Seppala, M., Depew, M. J., Martinelli, D. C., Fan, C. M., Sharpe, P. T. and Cobourne, M. T. (2007). Gas1 is a modifier for holoprosencephaly and genetically interacts with sonic hedgehog. *J. Clin. Invest.* **117**, 1575-1584.
Setkova, J., Matalova, E., Sharpe, P. T., Misek, I. and Tucker, A. S. (2007). Primary enamel knot cell death in Apaf-1 and caspase-9 deficient mice. *Arch. Oral. Biol.* **52**, 15-19.
Shigemura, N., Kiyoshima, T., Sakai, T., Matsuo, K., Momoi, T., Yamaza, H., Kobayashi, I., Wada, H., Akamine, A. and Sakai, H. (2001). Localization of activated caspase-3-positive and apoptotic cells in the developing tooth germ of the mouse lower first molar. *Histochem. J.* **33**, 253-258.
Soriano, P. (1999). Generalized lacZ expression with the ROSA26 Cre reporter strain. *Nat. Genet.* **21**, 70-71.
Trokovic, R., Trokovic, N., Hernesniemi, S., Pirvola, U., Vogt Weisenhorn, D. M., Rossant, J., McMahon, A. P., Wurst, W. and Partanen, J. (2003). FgfR1 is independently required in both developing mid- and hindbrain for sustained response to isthmic signals. *EMBO J.* **22**, 1811-1823.
Tucker, A. and Sharpe, P. (2004). The cutting-edge of mammalian development; how the embryo makes teeth. *Nat. Rev. Genet.* **5**, 499-508.
Tummers, M. and Thesleff, I. (2009). The importance of signal pathway modulation in all aspects of tooth development. *J. Exp. Zool. B Mol. Dev. Evol.* **312B**, 309-319.
Viriot, L., Lesot, H., Vonesch, J. L., Ruch, J. V., Peterka, M. and Peterkova, R. (2000). The presence of rudimentary odontogenic structures in the mouse embryonic mandible requires reinterpretation of developmental control of first lower molar histomorphogenesis. *Int. J. Dev. Biol.* **44**, 233-240.
Wang, X. P., O'Connell, D. J., Lund, J. J., Saadi, I., Kuraguchi, M., Turbe-Doan, A., Cavallesco, R., Kim, H., Park, P. J., Harada, H. et al. (2009). Apc inhibition of Wnt signaling regulates supernumerary tooth formation during embryogenesis and throughout adulthood. *Development* **136**, 1939-1949.
Weatherbee, S. D., Anderson, K. V. and Niswander, L. A. (2006). LDL-receptor-related protein 4 is crucial for formation of the neuromuscular junction. *Development* **133**, 4993-5000.
Yanagita, M., Okuda, T., Endo, S., Tanaka, M., Takahashi, K., Sugiyama, F., Kunita, S., Takahashi, S., Fukatsu, A., Yanagisawa, M. et al. (2006). Uterine sensitization-associated gene-1 (USAG-1), a novel Bmp antagonist expressed in the kidney, accelerates tubular injury. *J. Clin. Invest.* **116**, 70-79.
Yu, K., Xu, J., Liu, Z., Sosic, D., Shao, J., Olson, E. N., Towler, D. A. and Ornitz, D. M. (2003). Conditional inactivation of Fgf receptor 2 reveals an essential role for Fgf signaling in the regulation of osteoblast function and bone growth. *Development* **130**, 3063-3074.

Table S1. Summary of qPCR array analyses with *Wise*$^{-/-}$ and *Wise*$^{-/-}$ tooth germs at E13.5

WNT pathway			
Symbol	*t*-test	Fold up- or downregulation	Bad melt curves
	P value	Mut/Het	
Aes	0.8987	-1.01	
Apc	0.418	2.14	
Axin1	0.4787	1.07	
Bcl9	0.0454	1.16	
Btrc	0.6134	1.04	X
Ctnnbip1	0.119	1.22	
Ccnd1	0.785	-1.02	
Ccnd2	0.1834	1.07	
Ccnd3	0.7061	1.04	
Csnk1a1	0.0913	1.14	
Csnk1d	0.0265	1.11	
Csnk2a1	0.3442	1.04	
Ctbp1	0.7376	-1.02	
Ctbp2	0.0513	1.14	
Ctnnb1	0.5067	-1.08	
Daam1	0.2978	1.04	
Dixdc1	0.1689	1.14	
Dkk1	0.0004	2.55	
Dvl1	0.9307	-1.02	
Dvl2	0.4351	1.08	
Ep300	0.3204	1.09	
Fbxw11	0.0021	1.13	
Fbxw2	0.8136	-1.01	
Fbxw4	0.7935	-1.03	
Fgf4	0.0007	9.92	
Fosl1	0.6842	1.09	
Foxn1	0.0253	-1.88	
Frat1	0.1473	-1.5	
Frzb	0.0138	1.26	
Fshb	0.6535	1.14	
Fzd1	0.0424	1.25	
Fzd2	0.0292	1.15	
Fzd3	0.5725	1.03	
Fzd4	0.9706	-1	
Fzd5	0.2925	-1.07	
Fzd6	0.1736	-1.09	
Fzd7	0.0478	1.36	
Fzd8	0.8217	-1.03	
Gsk3b	0.4596	-1.09	
Jun	0.6722	1.04	
Kremen1	0.0205	1.19	
Lef1	0.0096	1.23	
Lrp5	0.0504	-1.15	
Lrp6	0.9653	1	
Myc	0.2148	1.12	
Nkd1	0.0045	1.19	
Nlk	0.8944	1.01	

Pitx2	0.9122	1.01	
Porcn	0.6168	-1.04	
Ppp2ca	0.1405	-1.14	
Ppp2r1a	0.9942	-1	
Ppp2r5d	0.2755	1.11	
Pygo1	0.8761	-1.02	
Rhou	0.686	-1.03	
Senp2	0.8471	-1.02	X
Sfrp1	0.3574	-1.21	
Sfrp2	0.6069	1.03	
Sfrp4	0.0558	1.18	
Slc9a3r1	0.8376	-1.04	
Sox17	0.8283	1.04	
T	0.0003	-1.63	X
Tcf3	0.25	1.18	
Tcf7	0.0647	1.25	
Tle1	0.0802	1.15	
Tle2	0.7404	1.04	
Wif1	0.0264	1.13	
Wisp1	0.5063	-1.06	
Wnt1	0.9394	1.03	
Wnt10a	0.7591	1.06	
Wnt11	0.1451	-1.11	
Wnt16	0.5427	-1.12	
Wnt2	0.872	-1.01	
Wnt2b	0.46	1.4	
Wnt3	0.1144	-1.48	X
Wnt3a	0.0055	-1.43	
Wnt4	0.3078	-1.15	
Wnt5a	0.0543	1.27	
Wnt5b	0.0735	1.13	
Wnt6	0.0087	-1.22	
Wnt7a	0.0042	-2.67	
Wnt7b	0.7014	-1.08	
Wnt8a	0.7722	1.09	
Wnt8b	0.9512	-1.02	
Wnt9a	0.5291	-1.11	
Gusb	0.0911	-1.14	
Hprt1	0.2562	1.06	
Hsp90ab1	0.0441	1.05	
Gapdh	0.4229	-1.05	
Actb	0.0265	1.07	
MGDC	0.9394	1.03	
RTC	0.7926	1.05	
PPC	0.7494	1.12	

Hedgehog pathway			
Symbol	*t*-test	Fold up- or downregulation	Bad melt curves
	P value	Mut/Het	
Bmp2	0.7926	-1.07	
Bmp4	0.7184	1.09	
Bmp5	0.7314	1.08	
Bmp6	0.3074	1.2	
Bmp7	0.2961	1.24	
Bmp8a	0.4948	-1.38	
Bmp8b	0.5831	-1.2	
Boc	0.4609	1.07	
Btrc	0.4659	1.15	X
Cdon	0.8099	1.07	
Cep76	0.8394	-1.03	
Crim1	0.7514	-1.13	
Csnk1a1	0.7837	1.07	X
Csnk1d	0.7536	-1.05	
Csnk1e	0.5019	-1.14	
Csnk1g1	0.921	1.03	
Csnk1g2	0.3993	1.19	
Ctnna1	0.842	-1.03	
Ctnnb1	0.9854	-1.01	
Dhh	0.8781	1.06	
Disp1	0.9551	1.01	
Erbb4	0.0023	-1.7	
Fbxw11	0.9817	1.01	
Fgf9	0.5259	1.11	
Fgfr3	0.4181	1.14	
Fkbp8	0.3935	-1.54	
Foxe1	0.5354	-1.37	
Gas1	0.8932	1.02	
Gli1	0.7273	1.12	
Gli2	0.5058	1.09	
Gli3	0.8004	-1.04	
Grem1	0.4332	-1.19	
Gsk3b	0.9419	1.02	
Hhat	0.5746	1.16	
Hhip	0.0522	1.52	
Ift52	0.9972	-1	
Ihh	0.787	1.11	
Kctd11	0.7302	1.16	
Lrp2	0.6216	-1.28	
Mapk1	0.743	1.06	
Mtss1	0.9973	-1	
Npc1	0.6721	-1.08	
Npc1l1	0.2922	-1.82	
Numb	0.9466	-1.01	
Otx2	0.5266	-1.09	
Prkaca	0.4264	1.17	
Prkacb	0.9288	1.02	
Prkx	0.7431	1.05	

Ptch1	0.1202	1.56	
Ptch2	0.0427	1.73	
Ptchd1	0.7611	1.09	
Ptchd2	0.0149	2.03	
Ptchd3	0.542	1.16	X
Rab23	0.9497	1.02	
Runx2	0.6328	1.11	
Sfrp1	0.57	1.13	
Shh	0.0156	3.32	
Shox2	0.7951	1.07	
Siah1a	0.9165	1.02	
Smo	0.8183	-1.04	
Stk36	0.9601	1.01	
Sufu	0.7458	1.08	
Wif1	0.4701	1.17	
Wnt1	0.8722	-1.02	X
Wnt10a	0.9998	1	
Wnt10b	0.4192	1.23	
Wnt11	0.3308	5.41	
Wnt16	0.5414	-1.25	
Wnt2	0.4928	1.57	
Wnt2b	0.4812	1.24	
Wnt3	0.7286	-1.11	
Wnt3a	0.0801	-1.33	
Wnt4	0.5992	-1.16	
Wnt5a	0.3486	1.64	
Wnt5b	0.4344	-1.1	
Wnt6	0.1729	-1.53	
Wnt7a	0.0302	-4.05	X
Wnt7b	0.979	-1.01	
Wnt8a	0.4976	1.18	X
Wnt8b	0.7134	-1.16	
Wnt9a	0.8065	1.12	
Wnt9b	0.2996	2.23	
Zic1	0.9956	1	X
Zic2	0.9545	-1.04	X
Gusb	0.4969	1.35	
Hprt1	0.782	1.04	
Hsp90ab1	0.294	-1.64	
Gapdh	0.9377	1.01	
Actb	0.5558	1.15	

Growth factors			
Symbol	*t*-test	Fold up- or downregulation	Bad melt curves
	P value	Mut/Het	
Amh	0.1358	1.69	
Artn	0.3351	-1.19	
Bdnf	0.6836	1.05	
Bmp1	0.7581	-1.02	
Bmp10	0.1358	1.69	
Bmp2	0.5366	1.04	
Bmp3	0.0333	-1.45	
Bmp4	0.2108	1.14	
Bmp5	0.331	-1.09	
Bmp6	0.8596	1.01	
Bmp7	0.865	-1.01	
Bmp8a	0.8437	1.08	
Bmp8b	0.0589	-1.44	
Csf1	0.5106	1.05	
Csf2	0.1358	1.69	
Csf3	0.1316	1.4	
Cxcl1	0.5102	-1.19	
Cxcl12	0.8807	1	
Egf	0.0548	-1.49	
Ereg	0.0526	2.09	
Fgf1	0.4617	1.16	
Fgf10	0.1169	-1.12	
Fgf11	0.8155	-1.03	
Fgf13	0.1858	1.06	
Fgf14	0.1965	-1.18	
Fgf15	0.0194	4.1	
Fgf17	0.4365	1.34	
Fgf18	0.0795	-1.39	
Fgf2	0.8009	1.03	
Fgf22	0.513	-1.14	
Fgf3	0	9.19	
Fgf4	0	9.7	
Fgf5	0.0919	2.71	
Fgf6	0.8738	1.07	
Fgf7	0.0758	-1.08	
Fgf8	0.4413	1.11	
Fgf9	0.5052	1.19	
Figf	0.3432	-1.18	
Gdf10	0.8126	-1.01	
Gdf11	0.653	1.01	
Gdf5	0.396	1.1	
Mstn	0.4754	-1.36	
Gdnf	0.8804	-1.04	
Hgf	0.1393	-1.2	
Igf1	0.0042	-1.15	
Igf2	0.0256	1.31	
Il11	0.2618	1.23	
Il12a	0.0518	2.06	

Il18	0.4439	1.18	
Il1a	0.984	-1.01	
Il1b	0.1855	1.5	
Il2	0.1171	1.72	
Il3	0.1358	1.69	
Il4	0.5426	1.09	
Il6	0.3578	1.16	
Il7	0.1358	1.69	
Inha	0.7553	-1.05	
Inhba	0.2481	-1.14	
Inhbb	0.9292	-1.03	
Kitl	0.0008	-1.08	
Lefty1	0.2568	1.21	
Lefty2	0.6332	-1.07	
Lep	0.1358	1.69	
Lif	0.6984	-1.13	
Mdk	0.1536	-1.19	
Ngf	0.084	1.12	
Nodal	0.0592	2.29	
Ntf3	0.0729	-1.24	
Ntf5	0.3615	-1.25	
Pdgfa	0.3558	-1.07	
Pgf	0.2995	1.1	
Rabep1	0.675	-1.03	
S100a6	0.0417	-1.34	
Spp1	0.0192	-1.92	
Tdgf1	0.0699	1.77	
Tff1	0.1358	1.69	
Tgfa	0.1605	1.29	
Tgfb1	0.032	1.2	
Tgfb2	0.2302	1.1	
Tgfb3	0.9465	-1.01	
Vegfa	0.7861	1.01	
Vegfb	0.5308	1.05	
Vegfc	0.3562	-1.05	
Zfp91	0.2901	-1.09	
Gusb	0.3328	-4.21	
Hprt1	0.2691	1.02	
Hsp90ab1	0.1589	1.05	
Gapdh	0.0312	-1.15	
Actb	0.0712	1.07	
MGDC	0.1423	-1.18	
RTC	0.158	1.34	
PPC	0.001	1.81	

Bmp/Tgfβ pathway			
Symbol	*t*-test	Fold up- or downregulation	Bad melt curves
	P value	Mut/Het	
Acvr1	0.121	1.13	
Acvr2a	0.0083	-1.12	
Acvrl1	0.5249	1.04	
Amh	0.4579	-1.1	
Amhr2	0.3337	-1.25	
Bambi	0.1385	1.3	
Bglap2	0.6448	-1.2	
Bmp1	0.7251	-1.02	
Bmp2	0.6397	1.12	
Bmp3	0.4127	-1.18	
Bmp4	0.5633	1.2	
Bmp5	0.4825	1.11	
Bmp6	0.4311	1.11	
Bmp7	0.1235	1.22	
Bmper	0.5192	1.12	
Bmpr1a	0.2916	-1.06	
Bmpr1b	0.8403	1.03	
Bmpr2	0.946	1	
Cd79a	0.8706	-1.04	
Cdc25a	0.2569	1.04	
Cdkn1a (p21)	0.0076	1.74	
Cdkn2b	0.8458	1.04	
Chrd	0.0542	1.29	X
Col1a1	0.1	1.3	
Col1a2	0.152	1.32	
Col3a1	0.3511	1.04	
Dlx2	0.0157	1.46	
Eng	0.9408	1.02	
Evi1	0.2843	-1.16	
Fkbp1b	0.6133	-1.08	
Fos	0.9564	-1.01	
Fst	0.0417	-1.25	
Gdf1	0.4912	1.14	
Gdf2	0.6223	1.17	
Gdf3	0.2245	-1.14	
Gdf5	0.4735	-1.18	
Gdf6	0.4944	-1.15	
Gdf7	0.5504	1.16	
Gsc	0.9483	-1	
Id1	0.8817	-1.01	
Id2	0.4249	-1.09	
Igf1	0.3483	-1.13	
Igfbp3	0.2548	1.13	
Il6	0.7039	1.29	
Inha	0.9817	1.01	
Inhba	0.2415	1.32	
Inhbb	0.4606	1.2	
Itgb5	0.8296	-1.03	

Itgb7	0.4724	1.12	
Jun	0.2519	-1.62	
Junb	0.4657	-1.17	X
Lefty1	0.4581	1.06	
Ltbp1	0.0912	1.15	
Ltbp2	0.5313	1.19	
Ltbp4	0.1343	1.12	
Myc	0.2345	-1.07	
Nbl1	0.452	-1.12	
Nodal	0.6423	1.19	
Nog	0.6538	-1.1	
Nr0b1	0.8584	1.08	
Pdgfb	0.9736	-1	
Plat	0.359	-1.27	
Plau	0.3325	-1.23	
Runx1	0.3197	1.12	
Serpine1	0.6859	1.27	
Smad1	0.5503	-1.07	
Smad2	0.764	-1.03	
Smad3	0.9089	1.01	
Smad4	0.4388	1.2	
Smad5	0.5804	-1.03	
Smurf1	0.6609	1.08	
Sox4	0.7789	1.12	
Stat1	0.0033	1.25	
Tdgf1	0.4579	-1.1	
Tgfb1	0.1054	1.3	
Tgfb1i1	0.3687	1.08	
Tsc22d1	0.3359	-1.14	
Tgfb2	0.2481	1.1	
Tgfb3	0.1691	1.19	
Tgfbi	0.4438	1.06	
Tgfbr1	0.4272	1.05	
Tgfbr2	0.7348	1.1	
Tgfbr3	0.9794	-1.01	
Tgfbrap1	0.9008	1.01	
Gusb	0.3188	-1.18	
Hprt1	0.2976	1.11	
Hsp90ab1	0.8899	-1.01	
Gapdh	0.8006	1.01	
Actb	0.6837	1.06	
MGDC	0.4579	-1.1	
RTC	0.2968	-1.2	
PPC	0.3954	-1.12	

Custom-designed assays			
Symbol	*t*-test	Fold up- or downregulation	Bad melt curves
	P value	Mut/Het	
Axin2	0.4513	1.09	
Rspo2	0.084	-1.15	
Etv4 (Pea3)	0.0042	2.31	
Etv5	0.1501	1.6	
Spry2	0.013	1.5	
Fgfr1	0.0243	1.68	
Eda	0.2573	1.06	
Edar	0.0841	1.77	X
Pax9	0.4105	1.07	
Msx2	0.4808	1.06	

Genes with more than 1.4-fold change ($P \leq 0.05$) are dark-shaded. Two genes, *Wnt3a* and *Bmp3*, were present in two different arrays and showed significant change only in one array. Genes with bad melt curves were excluded.